Korean J. Chem. Eng., 34(12), 3048-3053 (2017)
DOI: 10.1007/s11814-017-0227-6

pISSN: 0256-1115
eISSN: 1975-7220

Analysis of air blast effect for explosives in a large scale detonation

Hweeung Kwon*, Kyungjae Tak*, Sanjeev Maken*,, Hyounsoo Kim***, Jungsu Park***, and Il Moon*,†**

*Department of Chemical and Biomolecular Engineering, Yonsei University, 50 Yonsei-ro, Seodaemun-gu, Seoul 03722, Korea
**Department of Chemistry, Deenbandhu Chhotu Ram University of Science and Technology, Murthal-131 039, India
***The 4th R&D Institute-2 Agency for Defense Development, Daejeon 34186, Korea
(*Received 11 June 2015 • accepted 15 August 2017*)

Abstract−Open Burning/Open Detonation (OB/OD) has been widely used for demilitarization of expired explosives. However, OB/OD effects a variety of hazardous damages to environment. Therefore, using incinerators to treat expired explosives is required instead of OB/OD. To guarantee the safety of these demilitarization methods, the blast wave of the explosives should be previously recognized to evaluate the impact of detonations. Although various materials are used to produce explosives, most researches have focused on trinitrotoluene (TNT). Other representative explosives such as research department explosives (RDX) and high melting explosives (HMX) are seldom studied in the literature. Therefore, our aim was to understand the blast wave of three materials under different geometry throughout simulations. To improve accuracy and reduce computational time, a zoning technique with Euler-Lagrange coupling method was used. Due to limitations and difficulties of detonation experiments, simulations were verified by theoretical models. In case of semi-confined bunker, the simulation results were compared with experimental data, showing a close match. As a result, cylinder type is the safest incinerator among semi-confined bunker, cylinder, and cube incinerators, in terms of the blast wave.

Keywords: Explosion, Blast Effect, TNT, RDX, Detonation, Scaled Distance

INTRODUCTION

OB/OD techniques have been one of the most popular tools to demilitarize expired explosives for decades. However, OB/OD methods inherently contain the potential risk of detonation. In addition, detonation of explosives can cause massive damage of the environment by the blast wave. Therefore, many countries have developed and used various incinerators instead of OB/OD for demilitarization. Since safety is the most important factor in developing incinerators for demilitarization, it is required to analyze blast wave under various incinerator geometries.

It is very difficult to analyze a blast wave. Some researchers have conducted detonation experiments to study blast waves under different geometries and conditions. Baker [1] tested OD of TNT and analyzed the blast wave by a comparison of experimental and theoretical results [1]. Skacel et al. [2] considered detonation of condensed explosives inside shock tubes filled with different materials [2]. Chandra et al. [3] focused on dynamic pressure [3]. They obtained pressure-time profiles at various locations not only inside but also outside of a shock tube. Rigas and Sklavounos [4] detonated dense explosives in a complex tunnel structure [4]. Kowsarinia, Alizadeh, and Salavati Pour investigated underwater detonation of hexogen [5]. Because of many limitations to conduct detonation experiments of explosives, simulation becomes a reasonable approach that reduces risks, cost, and time to analyze the blast wave.

A TNT equivalent method, which calculates overpressure generated by various explosives by the TNT equivalent weight, has been widely used for explosion models [6]. A model with Euler has been used to analyze the propagation of the initial shock wave for a spherical charge of 1 kg TNT equivalent [7]. Mercx [8] analyzed the vapor cloud explosion with TNT equivalency and the multi-energy method in an offshore plant [8]. Liu [9] employed smoothed particle hydrodynamics for overpressure prediction [9]. Chapman et al. [10] developed 1- or 2-dimensional and time-dependent conservation equations [10]. Ning and Tang [11] simulated for a small-scale internal overpressure by the use of Livermore Software-DYNA [11]. Jo and Kim suggest method of explosion analysis based on explosion limit concentration in a confined area [12].

Previous studies have mainly focused on small-scale detonations of TNT. However, recent propellants have used explosives including RDX and HMX. Therefore, our aim was to predict the overpressure of TNT, RDX, and HMX in a large scale open detonation. The blast wave model embedded in ANSYS AUTODYN was employed and the maximum overpressures were validated with the experimental data. Detonation simulations were also carried out under different incinerator types: semi-confined bunker, cylinder, and tube.

This paper consists as follows. In section 2, the basic methodology of blast wave modeling is introduced. Section 3 verifies simulation results for OD by theoretical models, and section 4 compares with simulations and experiment dataset in semi-confined bunker. Section 5 describes the results of different incinerator types. The final section gives concluding remarks.

DETONATION OR BLAST WAVE MODELING

To simulate detonation of explosives, two different methods have

†To whom correspondence should be addressed.
E-mail: ilmoon@yonsei.ac.kr

Table 1. Physical and chemical properties of TNT, RDX, and HMX [16]

Physical and chemical properties	Information			
	TNT	RDX	HMX	Reference
Chemical formula	$C_7H_5N_3O_6$	$C_3H_6N_6O_6$	$C_4H_8N_8O_8$	Budavari et al., 1989; HSDB, 2009; HSDB, 1995
Molecular weight (g/mol)	227.13	222.26	296.17	Budavari et al., 1989; Merck, 1989; HSDB, 1995
Density at 20 °C (g/cm^3)	1.63	1.82	1.89	Budavari et al., 1989; Merck, 1989
Detonation velocity (m/s)	6900	8750	9100	-
Heat of detonation (MJ/kg)	4.55	5.98	6.04	Zhang and Chang, 2013
C_1 (Gpa)	3.730×10^2	7.828×10^2	7.782×10^2	
C_2 (Gpa)	3.747	13.35	7.071	
r_1	4.15	4.4	4.2	
r_2	0.9	1.288	1	ANSYS AUDYN
ω	0.35	0.32	0.3	
e (Gpa)	6	9.79	10.5	
Relative effectiveness factor	1	1.6	1.7	

been widely used: Euler and Lagrange. In the Euler region, the mesh is fixed in geometry and materials flow through the mesh. Therefore, this method enables treating a large amount of material flow and deformation of solid. However, it is not suitable for calculating the interface between fluid and solid. Contrary to the Euler method, the Lagrange method moves mesh and distorts by material motion. Thus, it is useful for interface calculation, but is difficult to handle large deformation of a solid. To take advantage of and to overcome disadvantages of each method, the Euler-Lagrange coupling method is employed in this study; Euler method calculates fluid motion and Lagrange method is used for structural materials.

The detonation consists of two steps. The first step calculates the initial expansion of explosives detonation with a 1-dimensional Euler method that considers radial symmetry to reduce simulation errors and guarantee accuracies. This result is, then, mapped onto the 2-dimensional geometry with zoning method in the second step. The zoning method refines the mesh in the critical regions. In general, the Lagrange method is simultaneously used in 2-dimensional geometry with Euler. Eq. (1) explains the mapping method to yield high resolution and grid in the first step of the blast wave expansion:

$$P=(\gamma-1)\rho e \tag{1}$$

where γ, e, and ρ are the specific heat ratio, internal energy, and density, respectively. The Jones-Wilkins-Lee (JWL) equation of state (EOS) is used for calculations of overpressures generated by detonations [13].

$$P=C_1\left(1-\frac{\omega}{r_1 v}\right)e^{r_1 v}+C_2\left(1-\frac{\omega}{r_2 v}\right)e^{r_2 v}+\frac{\omega e}{v} \tag{2}$$

where P, ω, v, and e are pressure, specific heat, specific volume, and detonation energy, respectively. C_1, C_2, r_1, and r_2 are material parameters and constants. Table 1 shows properties, parameters, and constants for TNT, HMX, and RDX [14,15]. The parameter and constant values in Table 1 can be applied for detonation simulations in the air.

OPEN DETONATION

The OD for demilitarization of expired explosives is one of the easiest methods. However, considering that explosives are detonated in an open area in OD method, the blast waves generated by detonation affect environment significantly. OD is simulated under various amounts of TNT, RDX, and HMX. It is assumed that the explosives exist at the center of the site and are detonated at ground level. The smaller the grid size, the higher accuracy and the more computational cost. Therefore, a zoning method is implemented to improve the simulation accuracy with computational time reduction; 1 cm for the grid size of Euler and Lagrange method is not applied OD because it do not exist structural materials.

The materials used for OD are air and explosives (TNT, RDX,

Table 2. Maximum overpressure in the OD cases

Distance	Simulation results								
	Pressure (kPa)								
	TNT			RDX			HMX		
	1 kg	2 kg	3 kg	1 kg	2 kg	3 kg	1 kg	2 kg	3 kg
2 m	604	762	918	778	979	1,184	887	1,110	1,330
4 m	103	147	189	257	366	499	287	389	517
6 m	42	58	98	109	159	222	117	175	245
8 m	28	38	46	59	85	120	62	88	132

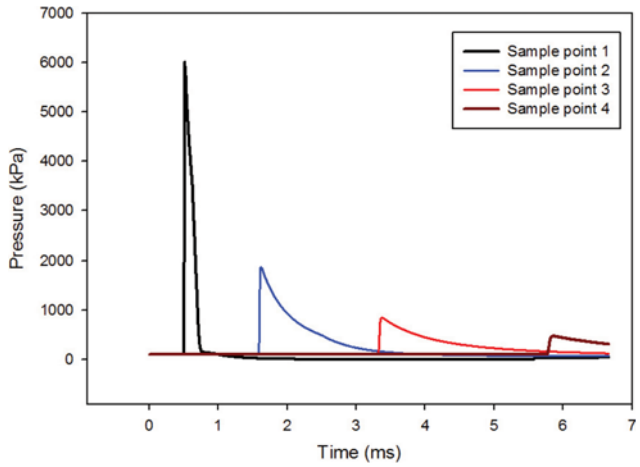

Fig. 1. Pressure-time profiles for OD of TNT.

and HMX). The OD simulation for of explosives has a mesh size of approximately 4,500,000. The indices for detonation performance are overpressure and impulse as dangerous factors [17]. We focused mainly on overpressure. The overpressures are measured at four sampling points in the geometry: two, four, six, and eight meters from the detonation point. The result is shown in Table 2. The order of maximum pressures measured at a distance of two meters is the same with the cases of detonation velocity and heat of detonation: from TNT (9,180 kPa) to RDX (11,840 kPa) and HMX (13,300 kPa).

Fig. 1 shows the overpressures as a function of time at the four sampling points for open detonation of TNT. The peaks at the points are attenuated rapidly. Moreover, the arrival time gap of the blast wave between neighbor sampling points becomes larger along with the distance, showing that blast propagation velocity becomes slower.

In the literature, there is a theoretical model that represents the relationship between scaled overpressure and scaled distance for TNT detonation. The definition of scaled overpressure is expressed in Eq. (5) and calculated by Eq. (6) [18,19]. Kinney and Graham detonated TNT and established Eq. (6) based on the result of TNT detonations.

$$P_s = \frac{P_o}{P_a} \tag{5}$$

$$\frac{P_o}{P_a} = \frac{1616\left[1+\left(\frac{Z_e}{4.5}\right)^2\right]}{\sqrt{\left[1+\left(\frac{Z_e}{0.048}\right)^2\right]\left[1+\left(\frac{Z_e}{0.32}\right)^2\right]\left[1+\left(\frac{Z_e}{1.35}\right)^2\right]}} \tag{6}$$

P_s, P_o, and P_a in Eq. (5) are the scaled overpressure (unitless), the peak side-on overpressure, and ambient pressure (1 atm), respectively. Z_e in Eq. (6) is the scaled distance and is defined with TNT mass and the distance, as shown in Eq. (7).

$$Z_e = \frac{r}{m_{TNT}^{1/3}}, \tag{7}$$

Fig. 2 illustrates the relationship not only for TNT but also for RDX and HMX. Substituting TNT mass to TNT equivalent mass

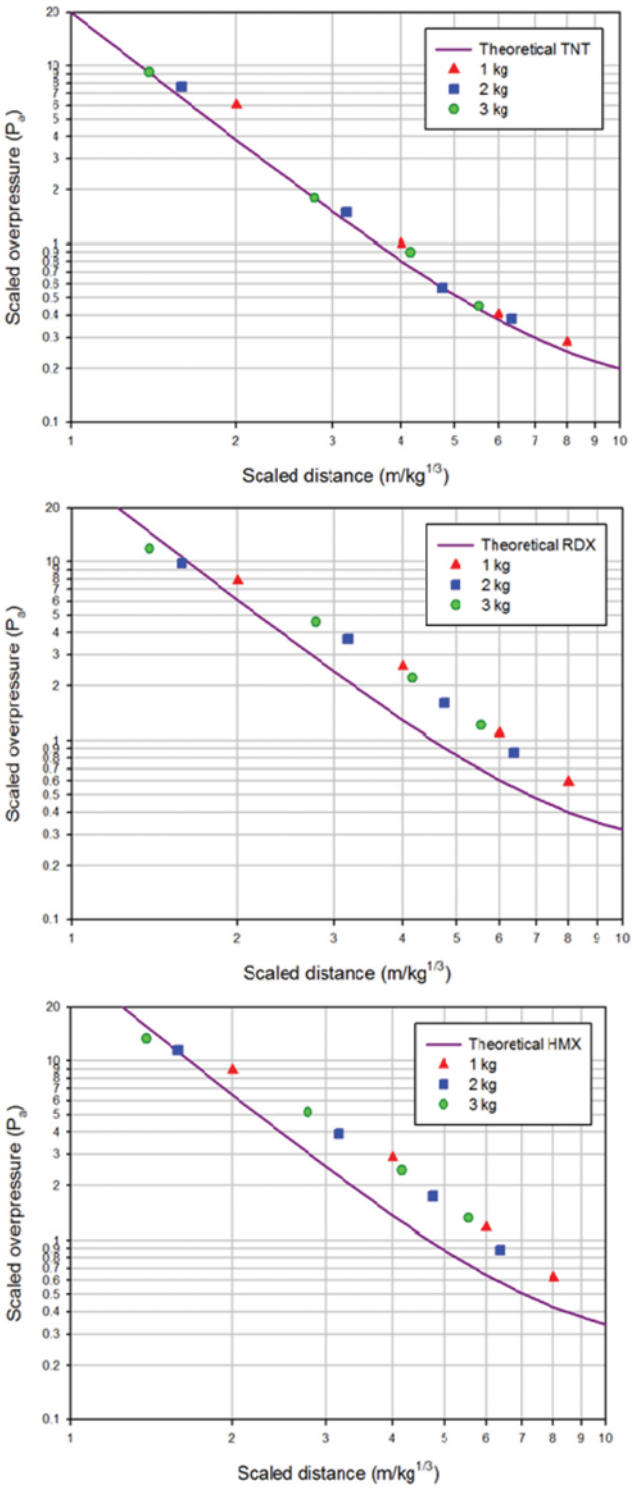

Fig. 2. The relationship between scaled overpressure and scaled distance for explosives.

is applied for RDX and HMX before using the theoretical model. The conversion factors of TNT equivalent mass for HMX and RDX are shown in Table 1. The drawing procedure for points of Fig. 2 is as follows: (1) Compute the overpressure of each explosives using the simulation, (2) Calculate scaled distance using the scaling law,

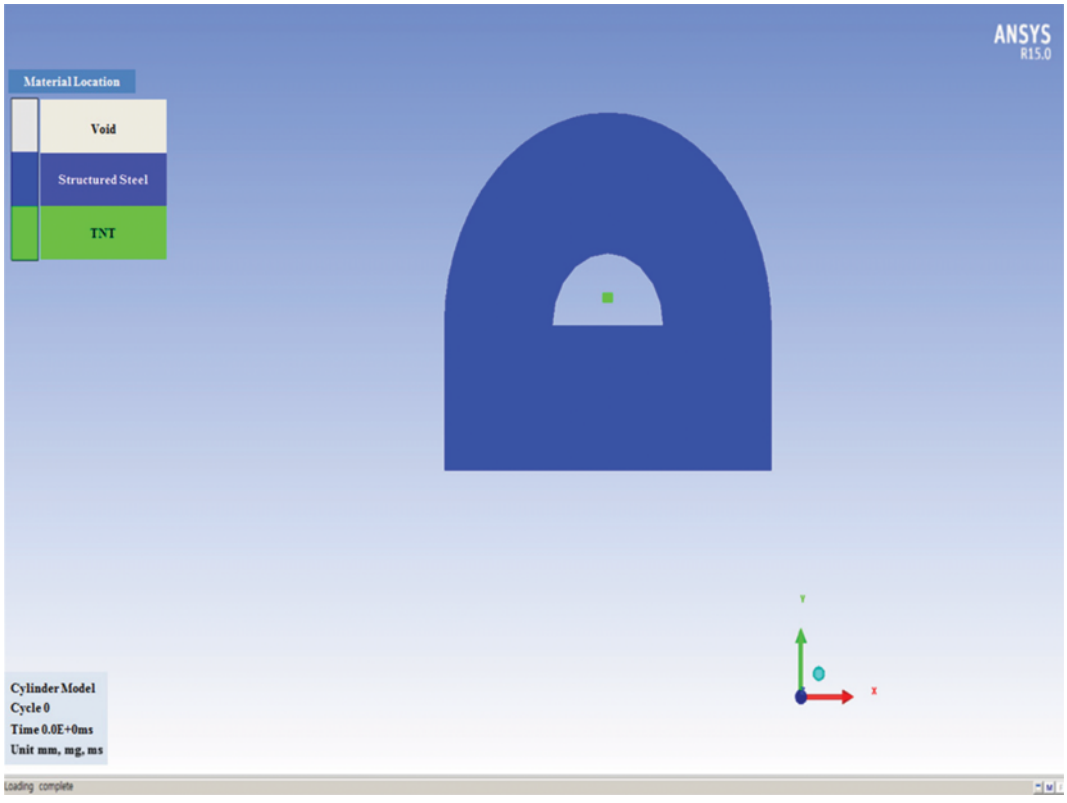

Fig. 3. Geometry of semi-confined bunker type with explosives.

Table 3. Maximum overpressure in the semi-confined bunker cases

Pressure (kPa)													
Distance	Experiment			Distance	Simulation results								
	TNT				TNT			RDX			HMX		
	1 kg	2 kg	3 kg		1 kg	2 kg	3 kg	1 kg	2 kg	3 kg	1 kg	2 kg	3 kg
5.37 m	181.28	261.52	424.75	5.37 m	179.93	267.83	492.23	220.85	332.86	621.64	234.65	352.36	649.60
5.37 m	176.71	240.83	387.97										
5.47 m	159.48	263.99	382.80	5.47 m	166.21	259.01	382.92	198.32	310.45	473.40	214.51	336.30	498.22
5.47 m	158.23	253.04	326.67										

(3) Put a point for overpressure values with scaled distance in graph (Fig. 2), and (4) Compare to simulation results and theoretical model. According to Fig. 2, these simulations are ground-burst with ground reflection effect, and it can be concluded that the trend relationship between scaled overpressure and scaled distance shows a close match with the theoretical model. The overpressure of RDX and HMX is bigger approximately 1.18 and 1.23 times than TNT.

DETONATION IN VARIOUS GEOMETRIES

To analyze the geometry effect on the blast wave, three semi-confined geometries are considered in this study: bunker, cylinder, and cube incinerators.

1. Semi-confined Bunker Type

The semi-confined bunker has its length of 20 m and radius of 1.8 m, as shown in Fig. 3. TNT, RDX, and HMX are located at the center of the semi-confined bunker. One, two, and three kg of explosives are used as the open detonation cases. Park and Lee studied explosion pressure effects of different ignition points by experiment [20]. In this study, two sampling points to measure overpressure exist at 5.37 m and 5.47 m away from the detonation point.

Table 3 shows the experiment and simulation results. The experiment was tested twice for each case of TNT detonation. Half of the results for TNT detonation simulation have an overpressure value in the range between two experimental results. The other overpressure values in the simulation such as 5.37 m for 2 kg TNT and 5.47 m for 1 kg TNT overestimate the experimental results. However, the experiment shows a large gap between twice-measured overpressure values; these seem to be acceptable.

In Table 3, although the increasing ratio of overpressure from 1 kg to 2 kg is different from that of overpressure from 2 kg to 3 kg

for all the explosives cases, there is little effect of explosives type on the trend. For instance, an overpressure at 5.37 m in the semi-confined bunker case is increased approximately 50% from 1 kg to 2 kg and 85% from 2 kg to 3 kg regardless of explosives types. This trend is similar to the experimental result. The overpressure in the semi-bunker type is approximately 9% decreased from 5.37 m to 5.47 m for 1 kg explosives, 5% decreased for 2 kg explosives, and 23% for 3 kg explosives.

2. Cylinder and Cube Types

Fig. 4 shows geometries for the cylinder and cube types. The length for these cases is 20 m, which is the same with the semi-confined bunker case. Radius of 1.8 m was used for the cylinder

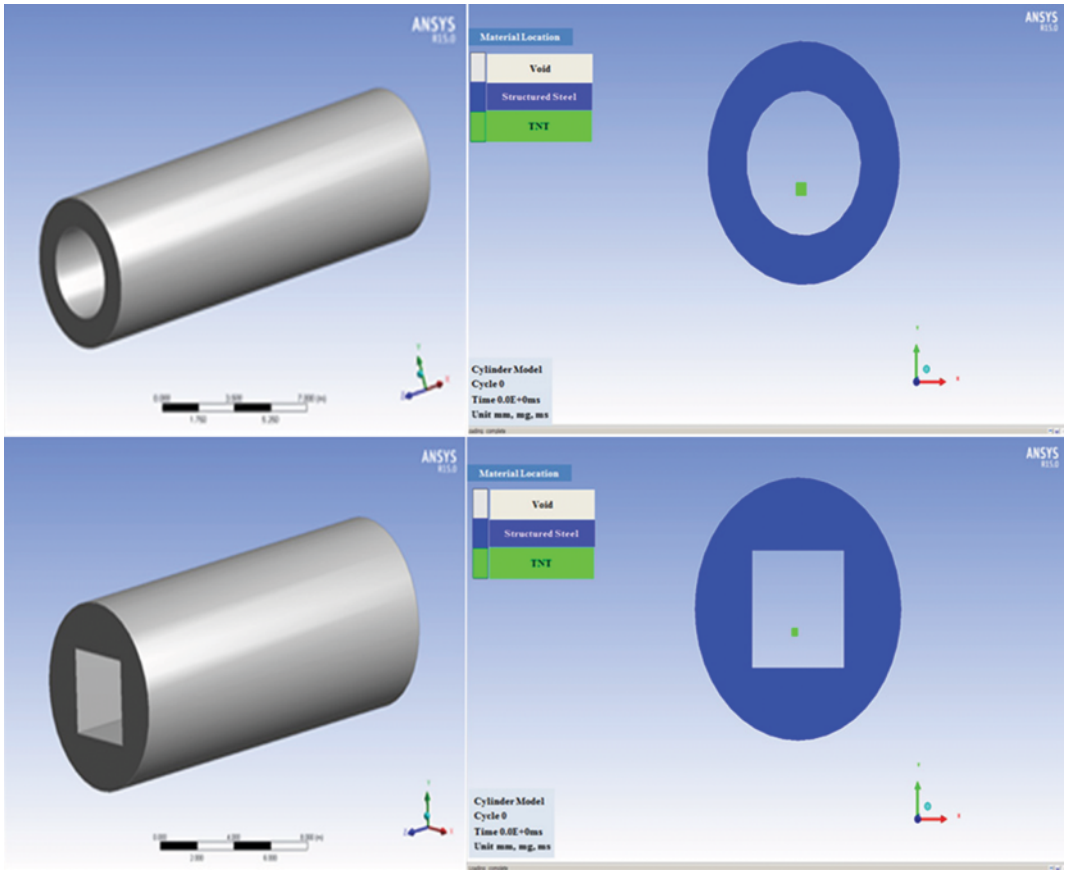

Fig. 4. Geometry of cylinder and cube types with explosives.

Table 4. Maximum overpressure in the cylinder cases

Distance	Simulation results								
	Pressure (kPa)								
	TNT			RDX			HMX		
	1 kg	2 kg	3 kg	1 kg	2 kg	3 kg	1 kg	2 kg	3 kg
5.37 m	98.31	159.91	240.37	116.93	190.85	289.17	124.19	205.20	312.10
5.47 m	60.13	132.14	166.24	70.97	144.86	198.54	75.71	169.11	214.80

Table 5. Maximum overpressure in the cube cases

Distance	Simulation results								
	Pressure (kPa)								
	TNT			RDX			HMX		
	1 kg	2 kg	3 kg	1 kg	2 kg	3 kg	1 kg	2 kg	3 kg
5.37 m	170.54	237.47	369.31	207.94	293.99	459.42	219.69	308.28	482.84
5.47 m	144.61	232.14	266.82	173.24	279.26	322.85	184.31	299.14	345.35

case. For the cube case, each side of 3.6 m was employed.

The results for cylinder and cube types are in Tables 4 and 5, respectively. Among three geometries, the cylinder type is the safest in terms of overpressure in comparison with the other two types. In general, the overpressure ratios are changed along with different geometries: about 63% increase from 1 kg to 2 kg and 51% from 2 kg to 3 kg for the cylinder type and 40% and 56% for the cube type. Moreover, the amount of explosives significantly affects decreasing ratio of overpressure at 5.37 m to overpressure at 5.48 m. As with the increasing ratio of overpressure by the amount of explosives, the decreasing ratio of overpressure by the distance has little relation to explosives type. Therefore, it is concluded that overpressure generated by RDX or HMX can reasonably well predict overpressure generated by TNT under the same amount of explosives and geometry.

CONCLUSION

To select a safe incinerator type, we focused on blast wave analysis for detonation of OD and various types. We analyzed blast wave to OD of TNT, RDX, and HMX, as compared with theoretical results. The R-squared values of the simulation results are 0.96-0.97 and it is concluded that the simulation shows a good performance. In addition, the model of the semi-confined bunker was simulated for explosives detonation and Euler-Lagrange coupling method was used. To take advantage of them simultaneously, the calculation results show a close match with experimental data. The blast wave ratios of TNT to RDX and TNT to HMX are 1 : 1.18-1.19 and 1 : 1.23-1.30, respectively. Furthermore, the detonation of three explosives was also tested for two other geometries: a cylinder and a cube. In general, the overpressures of semi-confined bunker, cylinder, and cube types are much higher than OD results due to geometry shapes. The blast wave in the cylinder is lower than semi-confined bunker and cube due to shock wave distribution. As a result, the incinerator of cylinder type is more safe than semi-confined bunker and cube types.

Finally, through the validation, the Euler-Lagrange coupling-based simulation produced reliable results and this method can be utilized to evaluate the safety of incinerator-based demilitarization. In the future work, the detonation of complex explosives will be simulated with the proposed geometries and identical environment.

ACKNOWLEDGEMENTS

The authors acknowledge the financial support of The Next-Generation Converged Energy Materials Research Center and Agency for Defense Development.

REFERENCES

1. W. E. Baker, Explosion in air, University of Texas, Austin, 150-163 (1973).
2. R. Skacel, B. Janovsky, L. Dostal and J. Svihovsky, *J. Loss Prev. Process Ind.*, **26**, 1590 (2013).
3. N. Chandra, S. Ganpule, N. N. Kleinschmit, R. Feng, A. D. Holmberg, A. Sundaramurthy, N. Selvan and A. Alai, *Shock Waves*, **22**, 403 (2012).
4. F. Rigas and S. Sklavounos, *J. Hazard. Mater.*, **A 121**, 23 (2005).
5. E. Kowsarinia, Y. Alizadeh and H. S. Salavati Pour, *IJE Transactions B: Applications*, **25**, 65 (2012).
6. F. D. Alonso, E. G. Ferradas, J. F. S. Perez, A. M. Aznar, J. R. Gimeno and J. M. Alonso, *J. Loss Prev. Process Ind.*, **19**, 724 (2006).
7. I. G. Cullis, *J R Army Med. Corps.*, **147**, 16 (2001).
8. W. P. M. Mercx, A. C. Van den Berg, C. J. Hayhurst, N. J. Robertson and K. C. Moran, *J. Hazard. Mater.*, **71**, 301 (2001).
9. M. B. Liu, G. R. Liu, Z. Zong and K. Y. Lam, *Comput. Fluids*, **32**, 305 (2003).
10. T. C. Chapman, T. A. Rose and P. D. Smith, *Int. J. Impact Eng.*, **16**, 777 (1997).
11. P. F. Ning and D. G. Tang, *J. Chongging Unversity*, **11**, 119 (2012).
12. Y. D. Jo and J. Y. Kim, *Korean J. Chem. Eng.*, **18**(3), 292 (2001).
13. G. Baudin and R. Serradeill, *EPJ Web of Conferences 10*, 00021 (2010).
14. X. Y. Wei, Z. Y. Zhao and J. Gu, *Int. J. Rock Mech. Min. Sci.*, **46**, 1206 (2009).
15. R. Jeremić and Z. Bajić, *Scientific-Technical Review*, **LVI**, 58 (2005).
16. J. Lee, J-H. Han, Y. Lee and H. Lee, *Int'I J. Aeronautical Space. Sci.*, **16**, 50 (2009).
17. S. G. Cho, K. T. No, E. M. Goh, J. K. Kim, J. H. Shin, Y. D. Joo and S. Seong, *Bull. Korean Chem. Soc.*, **26**, 399 (2005).
18. F. D. Alonso, E. G. Ferradas, J. F. S. Perez, A. M. Aznar, J. R. Gimeno and J. M. Alonso, *J. Hazard. Mater.*, **A137**, 734 (2006).
19. G. F. Kinney and K. J. Graham, Explosive shocks in air, Springer, Berlin (1985).
20. D. J. Park and Y. S. Lee, *Korean J. Chem. Eng.*, **29**(2), 139 (2012).